# The Highly Exothermic Hydrogen Abstraction Reaction $H_2Te + OH \rightarrow H_2O + TeH$: Comparison with Analogous Reactions for $H_2Se$ and $H_2S$

## Supporting Information

**Figure S1**. Profile of the CCSD(T) potential energy surface without zero-point vibrational energy (ZPVE) corrections for the $H_2Te + OH \rightarrow H_2O + TeH$ reaction. The 5Z results are single-point energies at the optimized QZ geometries (in kJ/mol).

**Figure S2**. Two possible pathways without ZPVE corrections for the $H_2Te + OH$ reaction. All energies are CCSD(T)/aug-cc-pV5Z-PP single point energies at the QZ optimized geometries (in kJ/mol).

**Figure S3**. Five stationary points on the potential energy surface for the $H_2Te + OH$ reaction. The single-point energies with 5Z at the optimized QZ geometries are corrected by ZPVE and spin-orbit coupling (SOC) effects (in kJ/mol).

**Figure S4**. Optimized geometries of the reactant complexes and the product complexes with two DFT (M06-2X and MPWB1K) functionals. All bond distances are in Å.

**Figure S5.** Comparison of the potential energy surface of the $H_2Te + OH$ reaction with the $H_2Se + OH$,[2] $H_2S + OH$,[3] and $H_2O + OH$[4] reactions at the CCSD(T)/5Z level (with ZPVE corrections, in kJ/mol).

**Figure S6.** Comparison of the potential energy surface of the $H_2Te + OH$ reaction with the $H_2Se + OH$,[2] $H_2S + OH$,[3] and $H_2O + OH$[4] reactions at the CCSD(T)/5Z level (without ZPVE corrections).

**Table S1.** $T_1$ diagnostic values of all the stationary points for the two pathways of the $H_2Te$ + OH reaction.

**Table S2**. Optimized geometries (Z-matrix) of the reactant (entrance) complex with the CCSD(T) method.

**Table S3**. Optimized geometries (Z-matrix) of the transition state **TS1** ($^2$A) and **TS2** ($^2$A") with the CCSD(T) method.

**Table S4**. Optimized geometries (Z-matrix) of the product (exit) complex with the CCSD(T) method.

**Table S5.** Harmonic vibrational frequencies ω ($cm^{-1}$) and infared intensities (km/mol, in parentheses) for the stationary points of the $H_2Te$ + OH reaction from the CCSD(T) method with the aug-cc-pV*n*Z-PP (*n* = D, T, Q) basis sets.

**Table S6.** Relative energies (kcal/mol) of the stationary points for the $H_2Te$ + OH reaction predicted by 28 DFT methods with the aug-cc-pVTZ-PP basis sets without ZPVE corrections.

**Table S7.** Predicted geometries for **TS1** by 28 DFT functionals with the aug-cc-pVTZ-PP basis sets.

**Table S8**. Barrier heights (in kcal/mol) using the CCSD(T)/aug-cc-pVQZ-PP single-point energies at the geometries predicted by the 28 DFT methods with the aug-cc-pVTZ-PP basis sets.

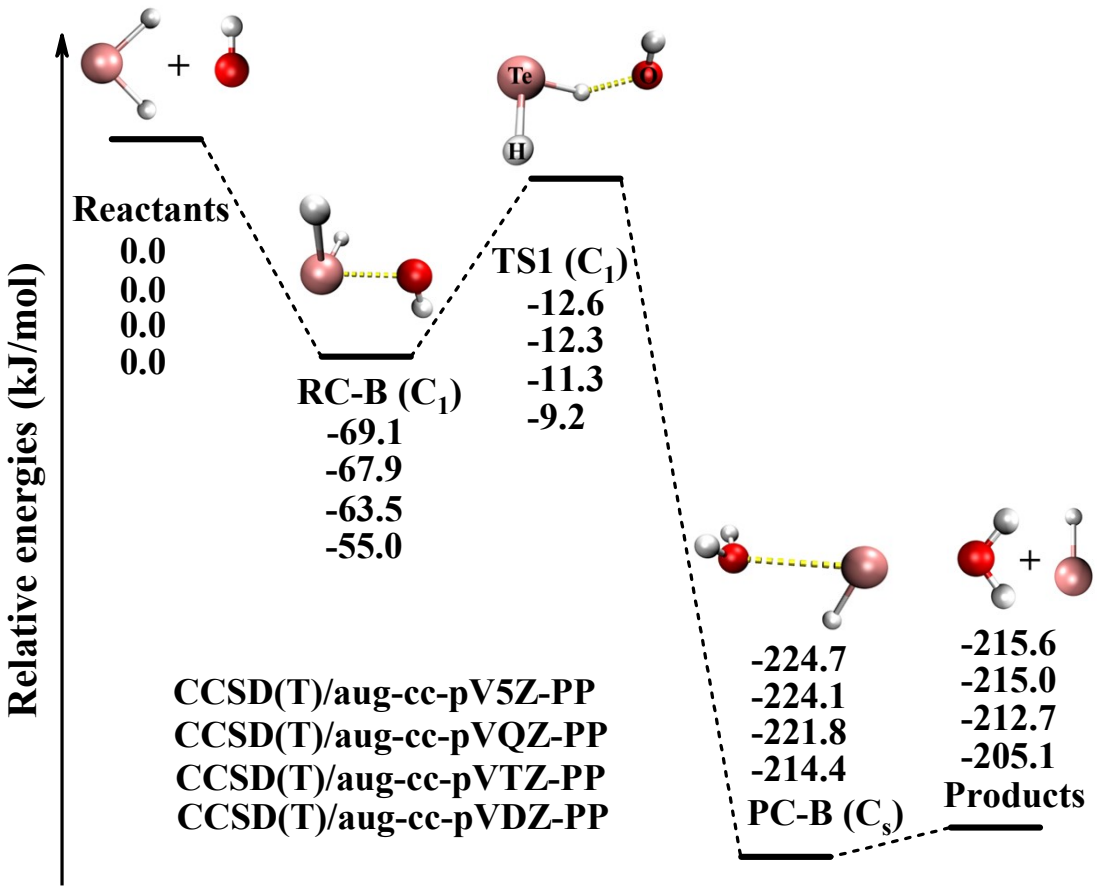


**Figure S1**. Profile of the CCSD(T) potential energy surface without zero-point vibrational energy (ZPVE) corrections for the $H_2Te + OH \rightarrow H_2O + TeH$ reaction. The 5Z results are single-point energies at the optimized QZ geometries (in kJ/mol).

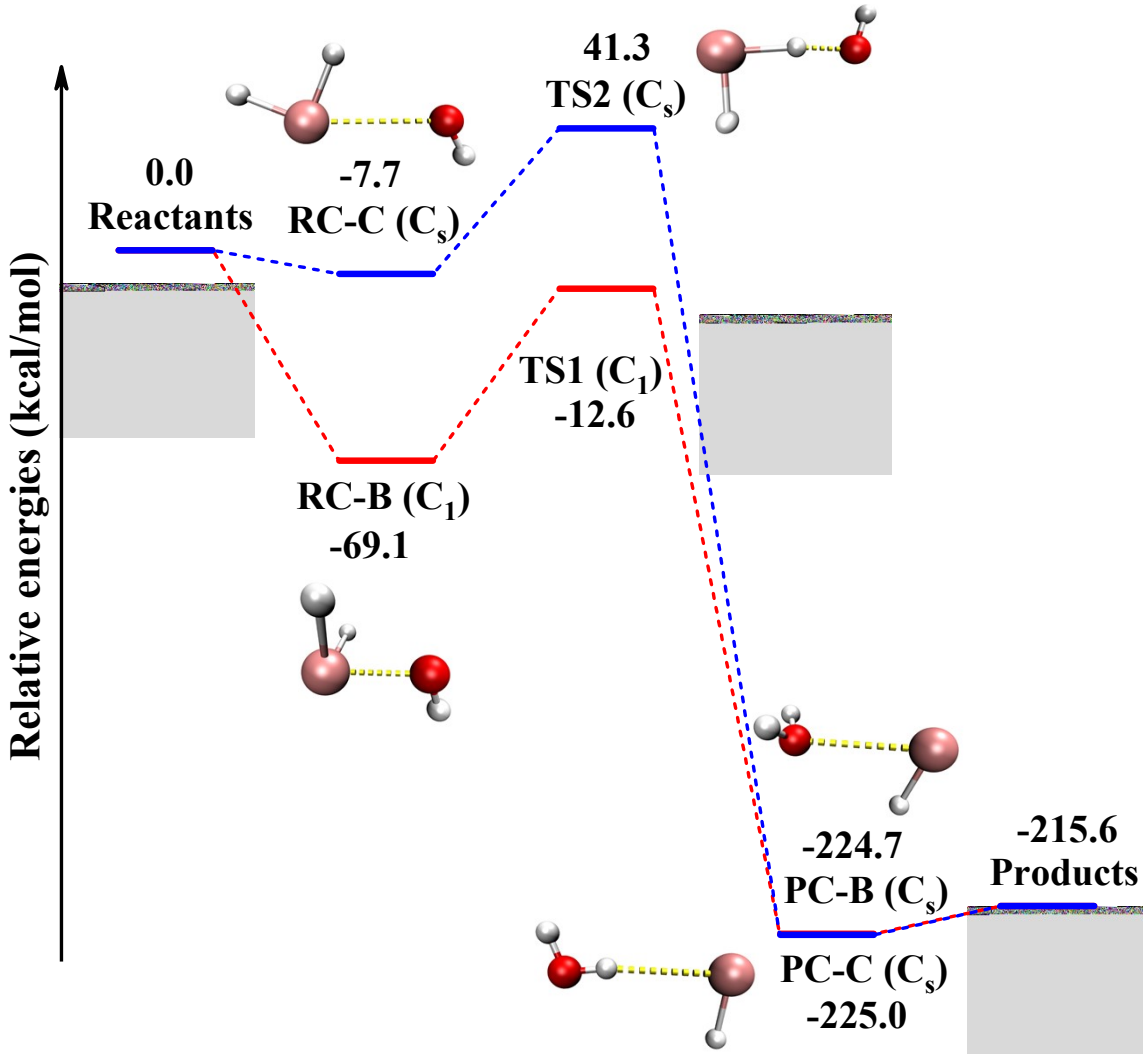


**Figure S2**. Two possible pathways without ZPVE corrections for the $H_2Te$ + OH reaction. All energies are CCSD(T)/aug-cc-pV5Z-PP single point energies at the QZ optimized geometries (in kJ/mol).

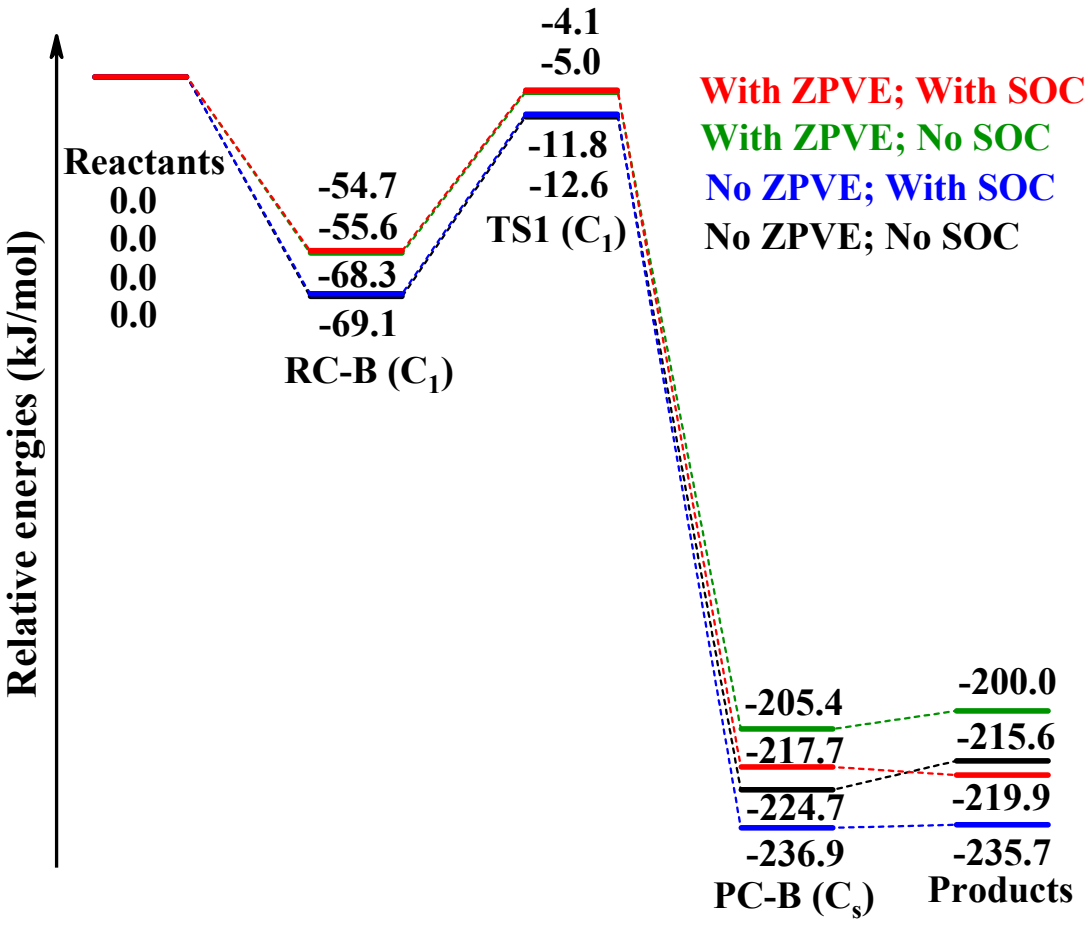


**Figure S3**. Five stationary points on the potential energy surface for the $H_2Te$ + OH reaction. The single-point energies with 5Z at the optimized QZ geometries are corrected by ZPVE and spin-orbit coupling (SOC) effects (in kJ/mol).

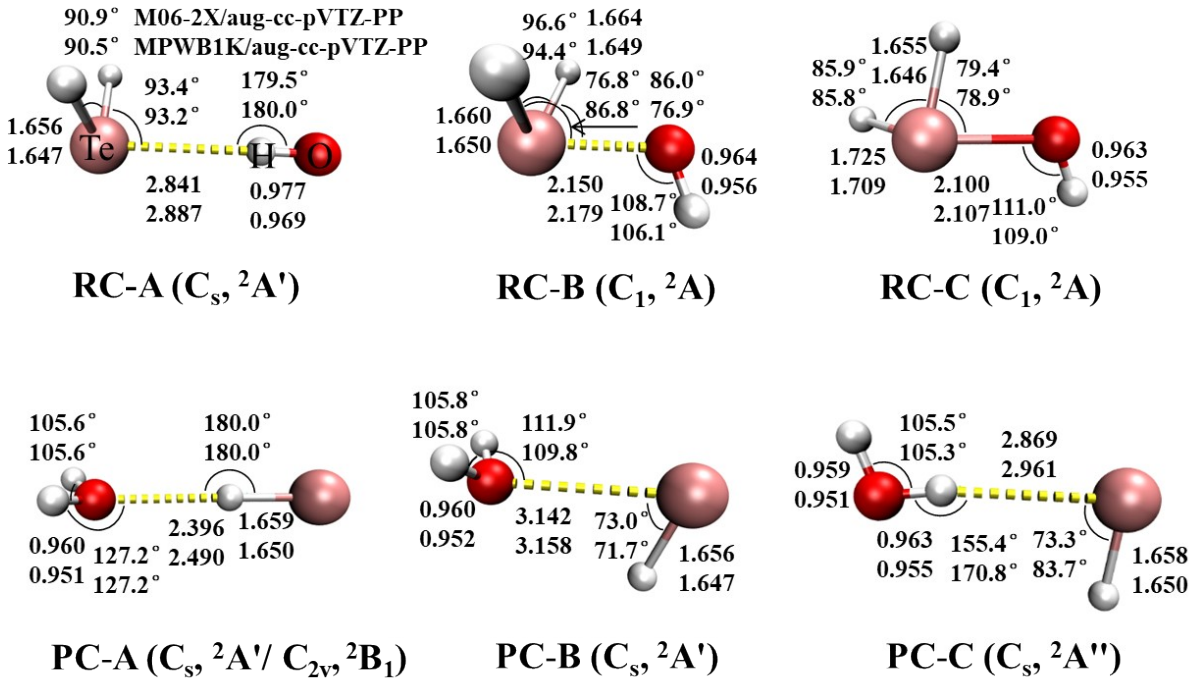


**Figure S4**. Optimized geometries of the reactant complexes and the product complexes with two DFT (M06-2X and MPWB1K) functionals. All bond distances are in Å.

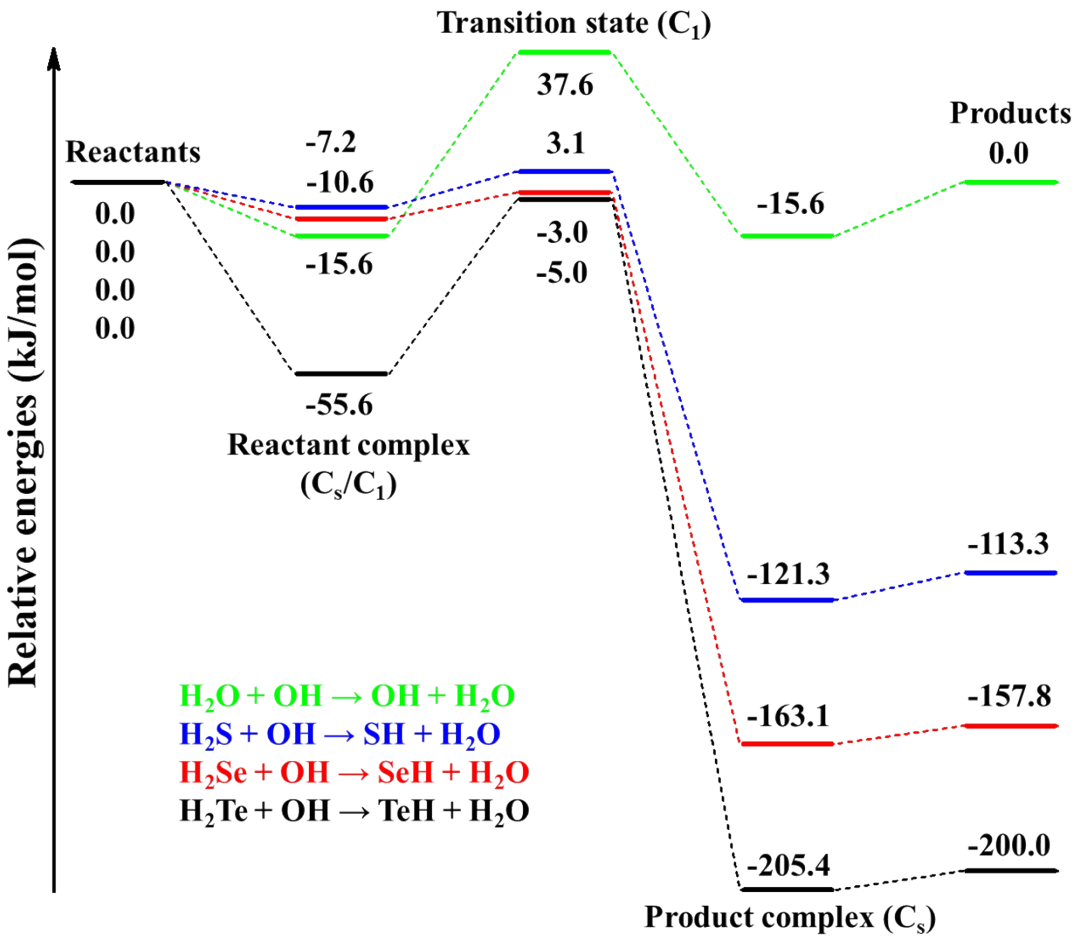


**Figure S5.** Comparison of the potential energy surface of the $H_2Te$ + OH reaction with the $H_2Se$ + OH,[2] $H_2S$ + OH,[3] and $H_2O$ + OH[4] reactions at the CCSD(T)/5Z level (with ZPVE corrections, in kJ/mol).

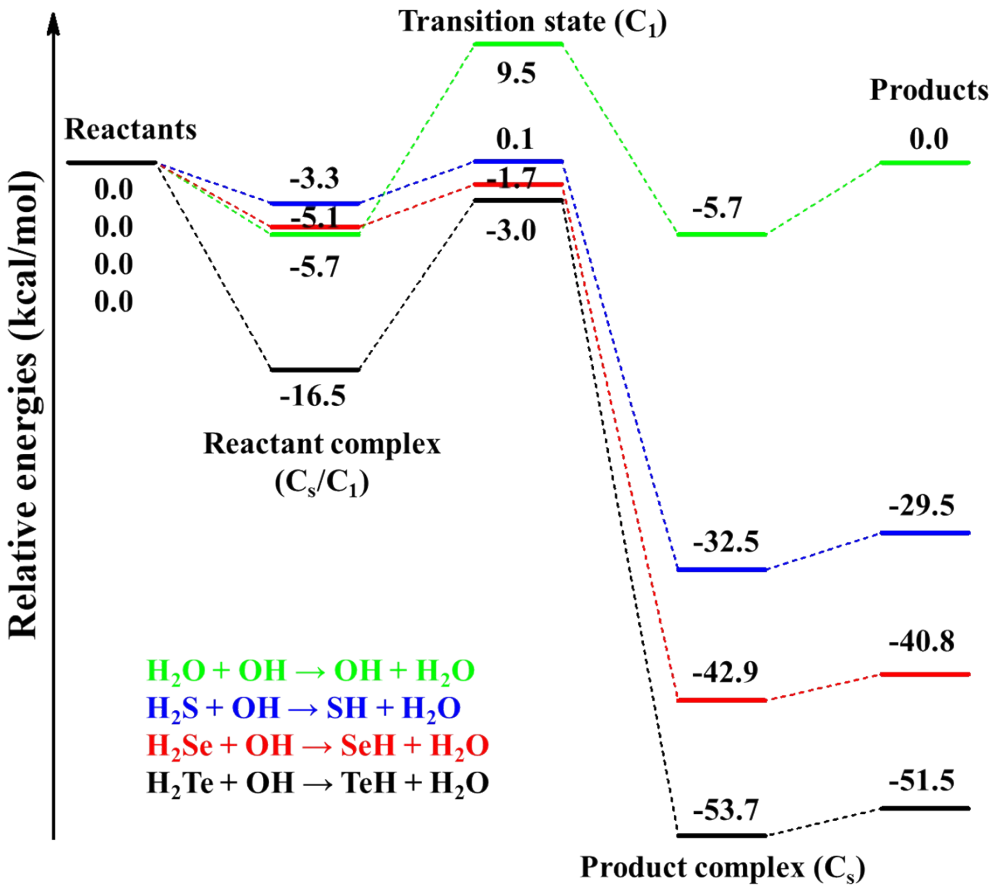


**Figure S6.** Comparison of the potential energy surface of the $H_2Te$ + OH reaction with the $H_2Se$ + OH,[2] $H_2S$ + OH,[3] and $H_2O$ + OH[4] reactions at the CCSD(T)/5Z level (without ZPVE corrections).

**Table S1.** $T_1$ diagnostic values of all the stationary points for the two pathways of the $H_2Te$ + OH reaction.

| | DZ | TZ | QZ | 5Z |
|---|---|---|---|---|
| **Path I** | | | | |
| **$H_2Te$** | 0.012 | 0.012 | 0.012 | 0.012 |
| **OH** | 0.017 | 0.014 | 0.014 | 0.013 |
| **RCB** | 0.038 | 0.030 | 0.029 | 0.029 |
| **TS1** | 0.072 | 0.076 | 0.080 | 0.080 |
| **PCB** | 0.018 | 0.016 | 0.016 | 0.016 |
| **$H_2O$** | 0.012 | 0.010 | 0.009 | 0.009 |
| **HTe** | 0.016 | 0.016 | 0.017 | 0.017 |
| | | | | |
| **Path II** | | | | |
| **RCC** | 0.019 | 0.018 | 0.018 | 0.018 |
| **TS2** | 0.088 | 0.082 | 0.082 | 0.081 |
| **PCC** | 0.018 | 0.016 | 0.016 | 0.015 |

**Table S2**. Optimized geometries (Z-matrix) of the reactant (entrance) complex with the CCSD(T) method. All bond distances are in Å, and angles are in degrees.

**RC-A** ($^2$A′)

| | aug-cc-pVDZ-PP | aug-cc-pVTZ-PP | aug-cc-pVQZ-PP |
|---|---|---|---|
| Te | B1 = 2.907518285157851 | B1 = 2.878324742479534 | B1 = 2.888760447092040 |
| H 1 B1 | B0 = 1.000000000500963 | B0 = 0.999999999792008 | B0 = 1.000000005162766 |
| X 2 B0 1 A0 | A0 = 88.98778929909377 | A0 = 90.297652401562587 | A0 = 90.037506754074258 |
| O 2 B2 3 A2 1 D2 | B2 = 0.983422332905190 | B2 = 0.977506869827624 | B2 = 0.974827836482296 |
| H 1 B3 2 A3 3 D3 | A2 = 88.96462520667931 | A2 = 90.274488116766534 | A2 = 90.014343972123200 |
| H 1 B3 2 A3 3 D4 | D2 = 180.0000000000000 | D2 = 180.000000000000000 | D2 = 180.000000000000000 |
| | B3 = 1.668057898514107 | B3 = 1.665067787395388 | B3 = 1.662099172800844 |
| | A3 = 91.942455036980547 | A3 = 93.151135560096535 | A3 = 93.335913097661290 |
| | D3 = -45.15323734103882 | D3 = -45.248478624702528 | D3 = -45.347599547446336 |
| | D4 = 45.15323734103882 | D4 = 45.248478624702528 | D4 = 45.347599547446336 |

**RC-B** ($^2$A)

| | aug-cc-pVDZ-PP | aug-cc-pVTZ-PP | aug-cc-pVQZ-PP |
|---|---|---|---|
| Te | B1 = 2.663193046283743 | B1 = 2.609969650369475 | B1 = 2.594105172331048 |
| H 1 B1 | B2 = 0.974273340206135 | B2 = 0.968373254063339 | B2 = 0.965896946616579 |
| O 2 B2 1 A2 | A2 = 53.549222391564825 | A2 = 52.951908215354386 | A2 = 52.612013499299110 |
| H 1 B3 2 A3 3 D3 | B3 = 1.671794482106665 | B3 = 1.672080470886669 | B3 = 1.670197945461297 |
| H 1 B4 2 A4 3 D4 | A3 = 96.482845250503871 | A3 = 96.670416423779258 | A3 = 96.791908973484610 |
| | D3 = -11.70845088797694 | D3 = -15.345433604678867 | D3 = -15.780800867767507 |
| | B4 = 1.671085452224168 | B4 = 1.668934873320940 | B4 = 1.666255105687253 |
| | A4 = 94.102491654825400 | A4 = 92.268412696604585 | A4 = 92.066693547754440 |
| | D4 = 81.76439139054635 | D4 = 79.608640902634377 | D4 = 79.687924541657509 |

**RC-C** ($^2$A″)

| | aug-cc-pVDZ-PP | aug-cc-pVTZ-PP | aug-cc-pVQZ-PP |
|---|---|---|---|
| Te | B1 = 1.671780349295196 | B1 = 1.668819695311005 | B1 = 1.665931009291979 |
| H 1 B1 | B2 = 1.664754025421492 | B2 = 1.661763947633245 | B2 = 1.658917799346088 |
| H 1 B2 2 A2 | A2 = 90.365658204236723 | A2 = 90.491223463219413 | A2 = 90.627957908752421 |
| O 3 B3 1 A3 2 D3 | B3 = 3.047894876423500 | B3 = 3.016925025100853 | B3 = 3.005042320503466 |
| H 4 B4 3 A4 1 D4 | A3 = 82.529553976466801 | A3 = 82.616312384029925 | A3 = 82.750952549820795 |
| | D3 = 180.0000000000000 | D3 = 180.000000000000000 | D3 = 180.000000000000000 |
| | B4 = 0.979800105097096 | B4 = 0.973850118908600 | B4 = 0.971217107609979 |
| | A4 = 153.29694608790103 | A4 = 149.864069866575250 | A4 = 150.091020428084306 |
| | D4 = 0.000000000000000 | D4 = 0.000000000000000 | D4 = 0.000000000000000 |

**Table S3**. Optimized geometries (Z-matrix) of the transition state **TS1** ($^2$A) and **TS2** ($^2$A") with the CCSD(T) method. All bond distances are in Å, and angles are in degrees.

**TS1** ($^2$A)

| | aug-cc-pVDZ-PP | aug-cc-pVTZ-PP | aug-cc-pVQZ-PP |
|---|---|---|---|
| Te<br>H 1 B1<br>O 2 B2 1 A2<br>H 3 B3 2 A3 1 D3<br>H 1 B4 2 A4 3 D4 | B1 = 1.692442082750316<br>B2 = 1.771025595432757<br>A2 = 104.740348053889733<br>B3 = 0.978490322458297<br>A3 = 106.271514842145507<br>D3 = -73.644876837823276<br>B4 = 1.665643230283776<br>A4 = 90.970868961365696<br>D4 = -71.776889029930771 | B1 = 1.692201559956625<br>B2 = 1.743486508383592<br>A2 = 101.051948297326135<br>B3 = 0.972185738793078<br>A3 = 105.698867342195953<br>D3 = -78.594456187845680<br>B4 = 1.662559146503983<br>A4 = 91.245578449706386<br>D4 = -71.405478866997782 | B1 = 1.692750081424527<br>B2 = 1.720418833841554<br>A2 = 99.211490093963633<br>B3 = 0.969339997558806<br>A3 = 105.835716423446442<br>D3 = -81.308500746895632<br>B4 = 1.659430572440181<br>A4 = 91.518737694681050<br>D4 = -71.622524691398041 |

**TS2** ($^2$A")

| | aug-cc-pVDZ-PP | aug-cc-pVTZ-PP | aug-cc-pVQZ-PP |
|---|---|---|---|
| Te<br>H 1 B1<br>X 2 B0 1 A0<br>O 2 B2 3 A2 1 D2<br>H 4 B3 2 A3 3 D3<br>H 1 B4 2 A4 3 D4 | B1 = 1.750531502528647<br>B0 = 0.984694529362742<br>A0 = 119.085369820963862<br>B2 = 1.518568367021253<br>A2 = 55.049552377815957<br>D2 = -180.000000000000000<br>B3 = 0.980087303955954<br>A3 = 106.239222328356405<br>D3 = -180.000000000000000<br>B4 = 1.669240936244411<br>A4 = 90.169122427541879<br>D4 = 0.000000000000000 | B1 = 1.748265616512917<br>B0 = 0.999752210812668<br>A0 = 90.927334298277586<br>B2 = 1.497998039766768<br>A2 = 84.165020871545252<br>D2 = 180.000000000000000<br>B3 = 0.974623687782766<br>A3 = 106.285967417189752<br>D3 = 180.000000000000000<br>B4 = 1.666447951493797<br>A4 = 90.355484962253456<br>D4 = 0.000000000000000 | B1 = 1.747057997924948<br>B0 = 0.999752415419339<br>A0 = 90.927334298277586<br>B2 = 1.492783971802241<br>A2 = 84.580113697790068<br>D2 = 180.000000000000000<br>B3 = 0.972008491542424<br>A3 = 106.432174958637574<br>D3 = 180.000000000000000<br>B4 = 1.663419394308638<br>A4 = 90.664437018739278<br>D4 = 0.000000000000000 |

**Table S4**. Optimized geometries (Z-matrix) of the product (exit) complex with the CCSD(T) method. All bond distances are in Å, and angles are in degrees.

**PC-A** ($^2$A′)

| | aug-cc-pVDZ-PP | aug-cc-pVTZ-PP | aug-cc-pVQZ-PP |
|---|---|---|---|
| O<br>H 1 B1<br>X 2 B0 1 A0<br>Te 2 B2 3 A2 1 D0<br>H 1 B3 2 A3 3 D3<br>H 1 B3 2 A3 3 D4 | B1 = 2.424355296203071<br>B0 = 0.999999999994735<br>A0 = 91.121041402958923<br>B2 = 1.672610459498500<br>A2 = 90.826921407841937<br>D0 = 180.0000000000000<br>B3 = 0.966664836656135<br>A3 = 123.72793043673959<br>D3 = -71.51373394703765<br>D4 = 71.513733947037650 | B1 = 2.401206266877878<br>B0 = 0.999999995995771<br>A0 = 90.147062320830088<br>B2 = 1.668494143824108<br>A2 = 89.852939905191775<br>D0 = 180.000000000000000<br>B3 = 0.961897348134964<br>A3 = 127.777554411414997<br>D3 = -90.000018749797690<br>D4 = 90.000018749797690 | B1 = 2.401194964039922<br>B0 = 0.999999995995771<br>A0 = 90.147062015950326<br>B2 = 1.665944109796990<br>A2 = 89.852939600325058<br>D0 = 180.000000000000000<br>B3 = 0.959265308334056<br>A3 = 127.692431280150018<br>D3 = -90.000018141764500<br>D4 = 90.000018141764500 |

**PC-B** ($^2$A′)

| | aug-cc-pVDZ-PP | aug-cc-pVTZ-PP | aug-cc-pVQZ-PP |
|---|---|---|---|
| O<br>H 1 B1<br>TE 2 B2 1 A2<br>H 1 B3 2 A3 3 D3<br>H 1 B3 2 A3 3 D4 | B1 = 3.084482609427815<br>B2 = 1.669889601669886<br>A2 = 80.958489902882718<br>B3 = 0.967036001268096<br>A3 = 127.0942480019109<br>D3 = -81.80919600773232<br>D4 = 81.80919600773232 | B1 = 3.035088586716309<br>B2 = 1.666048792447216<br>A2 = 81.066414326108116<br>B3 = 0.962305656596687<br>A3 = 126.414124984259786<br>D3 = -79.363044177934071<br>D4 = 79.363044177934071 | B1 = 3.038491006053379<br>B2 = 1.662937211500458<br>A2 = 80.749725200257757<br>B3 = 0.959695507845784<br>A3 = 126.307190733057212<br>D3 = -79.338624330602599<br>D4 = 79.338624330602599 |

**PC-**C ($^2$A″)

| | aug-cc-pVDZ-PP | aug-cc-pVTZ-PP | aug-cc-pVQZ-PP |
|---|---|---|---|
| O<br>H 1 B1<br>H 1 B2 2 A2<br>Te 3 B3 1 A3 2 D3<br>H 4 B4 3 A4 1 D4 | B1 = 0.966395462967040<br>B2 = 0.970330353426447<br>A2 = 103.96785995437518<br>B3 = 2.879778490052568<br>A3 = 166.44837713582367<br>D3 = 180.0000000000000<br>B4 = 1.672613622594432<br>A4 = 81.77196151055950<br>D4 = 0.000000000000000 | B1 = 0.961574230426386<br>B2 = 0.965358654082432<br>A2 = 104.216471654816885<br>B3 = 2.894573369050788<br>A3 = 167.957610879259249<br>D3 = 180.000000000000000<br>B4 = 1.668862486688320<br>A4 = 81.873250998601591<br>D4 = 0.000000000000000 | B1 = 0.958932075168831<br>B2 = 0.962539763415902<br>A2 = 104.409447510028016<br>B3 = 2.921601978905676<br>A3 = 166.994692968458054<br>D3 = 180.000000000000000<br>B4 = 1.665626078115529<br>A4 = 82.060203991158900<br>D4 = 0.000000000000000 |

**Table S5.** Harmonic vibrational frequencies ω ($cm^{-1}$) and infared intensities (km/mol, in parentheses) for the stationary points of the $H_2Te$ + OH reaction from the CCSD(T) method with the aug-cc-pV*n*Z-PP (*n* = D, T, Q) basis sets.

| | Vibrational Frequencies ω (Infrared Intensity) | | | | | | | | |
|---|---|---|---|---|---|---|---|---|---|
| | CCSD(T)/aug-cc-pV**D**Z-PP | | | | | | | | |
| $H_2Te$ + OH | 2141(46) | 2132(39) | 901(16) | ($H_2Te$); | | 3684(7) | (OH) | | |
| **RC-B** | 3722(15) | 2115(35) | 2084(28) | 863(42) | 835(13) | 601(4) | 325(32) | 308(27) | 156(29) |
| **TS1** | 3688(49) | 2145(25) | 1947(19) | 889(7) | 637(32) | 315(16) | 268(53) | 77(16) | 707i(2) |
| **PC-B** | 3898(56) | 3779(7) | 2121(46) | 1634(69) | 184(3) | 129(0) | 119(202) | 69(6) | 65(43) |
| $H_2O$+TeH | 3905(46) | 3787(2) | 1638(65) | ($H_2O$); | | 2110(49) | (TeH) | | |
| | CCSD(T)/aug-cc-pV**T**Z-PP | | | | | | | | |
| $H_2Te$ + OH | 2145(39) | 2137(34) | 887(14) | ($H_2Te$); | | 3718(10) | (OH) | | |
| **RC-B** | 3754(18) | 2112(33) | 2068(29) | 882(56) | 814(10) | 624(5) | 356(21) | 331(28) | 190(51) |
| **TS1** | 3724(58) | 2151(21) | 1954(4) | 872(5) | 663(25) | 349(16) | 292(53) | 107(12) | 802i(12) |
| **PC-B** | 3912(63) | 3802(10) | 2132(38) | 1642(73) | 201(3) | 127(1) | 122(207) | 73(5) | 71(40) |
| $H_2O$+TeH | 3920(54) | 3811(3) | 1646(70) | ($H_2O$); | | 2120(41) | (TeH) | | |
| | CCSD(T)/aug-cc-pV**Q**Z-PP | | | | | | | | |
| $H_2Te$ + OH | 2153(36) | 2146(31) | 885(14) | ($H_2Te$); | | 3739(11) | (OH) | | |
| **RC-B** | 3772(20) | 2118(32) | 2070(29) | 889(60) | 810(10) | 633(6) | 366(20) | 340(30) | 199(54) |
| **TS1** | 3744(62) | 2160(18) | 1951(1) | 870(5) | 678(22) | 370(15) | 308(53) | 130(8) | 866i(31) |
| **PC-B** | 3932(66) | 3821(11) | 2142(36) | 1646(74) | 202(2) | 125(1) | 121(210) | 72(6) | 70(41) |
| $H_2O$+TeH | 3941(58) | 3831(4) | 1650(72) | ($H_2O$); | | 2130(38) | (TeH) | | |

**Table S6.** Relative energies (kcal/mol) of the stationary points for the $H_2Te$ + OH reaction predicted by 28 DFT methods with the aug-cc-pVTZ-PP basis sets without ZPVE corrections. The most reliable CCSD(T)/5Z results are reported on the last line for comparison.

| Methods | $H_2Te$+OH | **RC-B** | **TS1** | Barrier of **TS1** from **RC-B** | **PC-B** | $H_2O$+HTe | HF% | Ref |
|---|---|---|---|---|---|---|---|---|
| BH&HLYP | 0.0 | −7.2 | −0.7 | 6.4 | −48.2 | −46.7 | 50 | 38 |
| MPW1K | 0.0 | −10.7 | −1.5 | 9.1 | −49.4 | −47.9 | 42.8 | 24 |
| MPWKCIS1K | 0.0 | −11.5 | −2.1 | 9.4 | −51.5 | −50.0 | 41 | 39 |
| BB1K | 0.0 | −12.5 | −2.5 | 10.1 | −50.6 | −49.2 | 42 | 40 |
| MPWB1K | 0.0 | −13.0 | −2.9 | 10.2 | −51.2 | −49.3 | 44 | 41 |
| M05-2X | 0.0 | −14.7 | −3.5 | 11.3 | −59.0 | −55.9 | 56 | 42 |
| M06-2X | 0.0 | −16.4 | −3.3 | 13.1 | −61.6 | −58.4 | 54 | 43 |
| BMK | 0.0 | −16.0 | −4.3 | 11.7 | −53.4 | −51.7 | 42 | 44 |
| ωB97-X | 0.0 | −15.4 | −4.2 | 11.2 | −53.0 | −49.4 | LC[a] | 45 |
| ωB97 | 0.0 | −15.3 | −3.9 | 11.4 | −52.8 | −48.8 | LC[a] | 45 |
| CAM-B3LYP | 0.0 | −15.2 | −4.8 | 10.4 | −52.4 | −50.5 | 19−65 | 46 |
| ωB97-XD | 0.0 | −15.2 | −4.9 | 10.4 | −52.3 | −49.6 | LC[a] | 47 |
| mPW1PW91 | 0.0 | −18.7 | −6.0 | 12.6 | −50.8 | −49.2 | 25 | 48,49 |
| M05 | 0.0 | −20.1 | −6.9 | 13.2 | −52.9 | −50.0 | 28 | 50 |
| PBE0 | 0.0 | −19.9 | −7.1 | 12.7 | −51.6 | −49.5 | 25 | 51-53 |
| B3PW91 | 0.0 | −19.6 | −7.2 | 12.4 | −50.9 | −49.8 | 20 | 49,54 |
| B3LYP | 0.0 | −19.2 | −7.3 | 11.9 | −51.0 | −49.5 | 20 | 54 |
| HSEh1PBE | 0.0 | −19.8 | −7.4 | 12.4 | −51.1 | −48.8 | 25 | 55-61 |
| B98 | 0.0 | −20.1 | −7.7 | 12.3 | −52.5 | −50.2 | 21.98 | 62 |
| MPW3LYP | 0.0 | −19.9 | −7.9 | 12.0 | −51.7 | −49.5 | 21.8 | 41,48 |
| TPSSh | 0.0 | −21.1 | −8.4 | 12.7 | −47.5 | −45.5 | 10 | 63 |
| M06 | 0.0 | −20.9 | −8.4 | 12.5 | −53.3 | −49.7 | 27 | 43 |
| TPSS1KCIS | 0.0 | −21.2 | −8.6 | 12.6 | −49.5 | −47.6 | 13 | 64 |
| MPW1KCIS | 0.0 | −22.3 | −10.6 | 11.7 | −53.5 | −51.8 | 15 | 39 |
| M06-L | 0.0 | −23.3 | −10.6 | 12.7 | −49.5 | −46.1 | 0 | 65 |
| VSXC | 0.0 | −22.7 | −13.1 | 9.7 | −55.6 | −49.8 | 0 | 66 |
| BLYP | 0.0 | −25.1 | −14.2 | 10.9 | −51.7 | −50.1 | 0 | 67,68 |
| BP86 | 0.0 | −27.3 | −16.0 | 11.3 | −53.1 | −51.0 | 0 | 68,69 |
| CCSD(T)/5Z | 0.0 | −16.5 | −3.0 | 13.5 | −53.7 | −51.5 | — | — |

[a]For the LC methods, the percentage of H-F component varies with the long-range corrections.

**Table S7.** Predicted geometries for **TS1** by 28 DFT functionals with the aug-cc-pVTZ-PP basis sets. Distances are in Angstrom, and angles are in degrees.

| Methods | R(H-Te) | R(Te··H) | R(H··O) | R(O-H) | ∠H-Te··H | ∠Te··H··O | ∠H··O-H | D(H-Te-H-O) | D(Te-H-O-H) |
|---|---|---|---|---|---|---|---|---|---|
| BH&HLYP | 1.6492 | 1.6774 | 1.7097 | 0.9617 | 91.2 | 143.9 | 101.6 | -85.5 | -2.8 |
| MPW1K | 1.6479 | 1.6650 | 1.8201 | 0.9623 | 91.0 | 123.8 | 105.7 | -81.3 | -17.8 |
| MPWKCIS1K | 1.6496 | 1.6689 | 1.8086 | 0.9616 | 91.3 | 112.8 | 108.5 | -73.5 | -52.5 |
| BB1K | 1.6453 | 1.6733 | 1.7351 | 0.9615 | 91.1 | 108.6 | 106.8 | -70.9 | -66.2 |
| MPWB1K | 1.6443 | 1.6715 | 1.7381 | 0.9610 | 91.1 | 110.3 | 106.9 | -70.6 | -61.8 |
| M06-2X | 1.6558 | 1.6793 | 1.7807 | 0.9717 | 90.9 | 127.6 | 104.1 | -79.9 | -13.8 |
| M05-2X | 1.6520 | 1.6715 | 1.8302 | 0.9696 | 91.1 | 121.7 | 104.7 | -74.3 | -26.4 |
| ωB97 | 1.6493 | 1.6670 | 1.8180 | 0.9721 | 91.3 | 123.7 | 104.7 | -79.5 | -19.4 |
| ωB97X | 1.6509 | 1.6787 | 1.7404 | 0.9677 | 91.7 | 106.3 | 107.3 | -71.6 | -71.0 |
| BMK | 1.6564 | 1.6887 | 1.7165 | 0.9662 | 91.5 | 102.0 | 107.6 | -72.2 | -80.6 |
| CAM-B3LYP | 1.6513 | 1.6776 | 1.7440 | 0.9687 | 91.7 | 102.7 | 108.1 | -72.5 | -77.3 |
| ωB97XD | 1.6539 | 1.6836 | 1.7330 | 0.9662 | 91.6 | 102.6 | 107.3 | -72.2 | -79.1 |
| mPW1PW91 | 1.6546 | 1.6820 | 1.7540 | 0.9663 | 91.4 | 99.9 | 106.9 | -72.8 | -81.1 |
| M05 | 1.6696 | 1.7123 | 1.6674 | 0.9644 | 91.6 | 101.9 | 106.4 | -71.4 | -88.0 |
| PBE0 | 1.6560 | 1.6842 | 1.7505 | 0.9672 | 91.4 | 98.8 | 106.9 | -72.7 | -82.2 |
| B3PW91 | 1.6576 | 1.6858 | 1.7596 | 0.9684 | 91.4 | 98.7 | 106.7 | -73.3 | -83.5 |
| B3LYP | 1.6612 | 1.6885 | 1.7660 | 0.9701 | 91.3 | 102.2 | 107.1 | -73.3 | -82.2 |
| HSEh1PBE | 1.6579 | 1.6862 | 1.7533 | 0.9672 | 91.4 | 99.6 | 106.9 | -72.7 | -81.7 |
| B98 | 1.6577 | 1.6846 | 1.7648 | 0.9684 | 91.4 | 100.9 | 107.0 | -73.0 | -82.0 |
| MPW3LYP | 1.6603 | 1.6878 | 1.7607 | 0.9696 | 91.4 | 102.2 | 107.4 | -72.9 | -81.8 |
| TPSSh | 1.6577 | 1.6902 | 1.7436 | 0.9728 | 91.0 | 99.8 | 105.2 | -72.1 | -85.1 |
| M06 | 1.6657 | 1.7071 | 1.6628 | 0.9662 | 90.7 | 104.4 | 105.8 | -70.2 | -84.6 |
| TPSS1KCIS | 1.6581 | 1.6907 | 1.7436 | 0.9708 | 91.1 | 99.8 | 105.9 | -72.5 | -85.3 |
| MPW1KCIS | 1.6632 | 1.6925 | 1.7766 | 0.9702 | 91.3 | 96.5 | 107.0 | -73.8 | -86.2 |
| M06-L | 1.6622 | 1.7093 | 1.6686 | 0.9670 | 90.1 | 106.0 | 104.0 | -70.6 | -87.8 |
| VSXC | 1.6603 | 1.7040 | 1.7338 | 0.9682 | 89.0 | 103.3 | 103.8 | -66.6 | -88.4 |
| BLYP | 1.6759 | 1.7051 | 1.8199 | 0.9801 | 91.0 | 97.6 | 106.3 | -74.1 | -88.8 |
| BP86 | 1.6715 | 1.7016 | 1.8097 | 0.9795 | 91.1 | 93.7 | 106.0 | -73.7 | -89.1 |
| CCSD(T)/QZ | 1.6594 | 1.6928 | 1.7204 | 0.9693 | 91.5 | 99.2 | 105.8 | -71.6 | -81.3 |

**Table S8.** Barrier heights (in kcal/mol) using the CCSD(T)/aug-cc-pVQZ-PP single-point energies at the geometries predicted by 28 DFT functionals with the aug-cc-pVTZ-PP basis sets.

| Methods for geometry optimization | Barrier height | Barrier of **TS1** from **RC-B** |
|---|---|---|
| BH&HLYP | −2.31 | 13.35 |
| MPW1K | −2.42 | 13.67 |
| MPWKCIS1K | −2.57 | 13.42 |
| BB1K | −2.78 | 13.30 |
| MPWB1K | −2.74 | 13.37 |
| M06-2X | −2.45 | 13.72 |
| M05-2X | −2.46 | 13.69 |
| ωB97 | −2.45 | 13.40 |
| ωB97X | −2.82 | 13.08 |
| BMK | −2.89 | 13.11 |
| CAM-B3LYP | −2.86 | 13.04 |
| ωB97XD | −2.86 | 12.95 |
| mPW1PW91 | −2.92 | 15.64 |
| M05 | −2.95 | 13.21 |
| PBE0 | −2.95 | 15.64 |
| B3PW91 | −2.94 | 15.53 |
| B3LYP | −2.77 | 15.34 |
| HSEh1PBE | −2.92 | 15.60 |
| B98 | −2.86 | 15.50 |
| MPW3LYP | −2.79 | 15.40 |
| TPSSh | −2.92 | 15.51 |
| M06 | −3.07 | 13.06 |
| TPSS1KCIS | −2.89 | 15.50 |
| MPW1KCIS | −2.99 | 15.29 |
| M06-L | −2.99 | 15.07 |
| VSXC | −2.65 | 14.89 |
| BLYP | −2.82 | 14.46 |
| BP86 | −3.16 | 14.84 |
| CCSD(T)/5Z | −3.01 | 13.52 |